Antinociceptive effect of N-(9,13b-dihydro-1H-dibenzo[c,f]imidazo[1,5-a]azepin-3-yl) -2-hydroxybenzamide on different pain models in mice

Hee-Jung Lee[1, 2], Hyun Min Lim,[3] Jing-Hui Feng[1, 2],
Ju Mi Lee,[3] Jeong Tae Lee,[3, *] Hong-Won Suh[1, 2, *]

[1]*Institute of Natural Medicine, Hallym University, Chuncheon 24252, Korea,*
[2]*Department of Pharmacology, College of Medicine, Hallym University, Chuncheon 24252, Korea,* [3]*Department of Chemistry and Institute of Applied Chemistry, College of Natural Sciences, Hallym University, Chuncheon 24252, Korea*

N-(9,13b-dihydro-1H-dibenzo[c,f]imidazo[1,5-a]azepin-3-yl)-2-hydroxybenzamide (DDIAHB) is a new drug developed through molecular modelling and rational drug design by the molecular association of epinastine and salicylic acid. The present study was designed to assess the possible antinociceptive effects of DDIAHB on different pain models in male ICR mice. DDIAHB exerted the reductions of writhing numbers and pain behavior observed during the second phase in the formalin test in a dose-dependent manner. Moreover, DDIAHB increased the latency in the hot-plate test in a dose-dependent manner. Furthermore, intragastric administration DDIAHB caused reversals of decreased pain threshold observed in both streptozotocin-induced diabetic neuropathy and vincristine-induced peripheral neuropathy models. Additionally, intragastric pretreatment with DDIAHB also caused reversal of decreased pain threshold observed in monosodium urate-induced pain model. We also characterized the possible signaling molecular mechanism of the antinociceptive effect-induced by DDIAHB in the formalin model. DDIAHB caused reductions of spinal iNOS, p-STAT3, p-ERK and p-P38 levels induced by formalin injection. Our results suggest that DDIAHB shows an antinociceptive property in various pain models. Moreover, the antinociceptive effect of DDIAHB appear to be mediated by the reductions of the expression of iNOS, p-STAT3, p-ERK and p-P38 levels in the spinal cord in the formalin-induced pain model.

Keywords: N-(9,13b-dihydro-1H-dibenzo[c,f]imidazo[1,5-a]azepin-3-yl)-2-hydroxybenzamide (DDIAHB). Antinociception. Spinal cord. Signal molecules.

INTRODUCTION

Epinastine (9,13b-dihydro-1H-dibenzo[c,f] imidazo[1,5-a]azepin-3-amine) is known as a histamine 1 receptor antagonist (Adamus, Oldigs-Kerber, Lohmann, 1987). Epinastine has been mostly used as an antiallergic drug, especially as an eyedrop form (Lanier *et al.*, 2004;

Mah *et al.*, 2007). The main antiallergic mechanism of epinastine was revealed in that a few cytokines such as interleukin 31 (IL-31), interleukin 8 (IL-8), and interleukin 4 (IL-4) are associated with the action of epinastine (Kanai *et al.*, 2006; Kohyama *et al.*, 1997; Mizuguchi *et al.*, 2009; Otsuka *et al.*, 2011a). Those cytokines are also involved in the regulation of chronic pain or pruritis (Hung, Lim, Doshi, 2017; Khan *et al.*, 2017; Mollanazar, Smith, Yosipovitch, 2016; Otsuka *et al.*, 2011b).

Salicylic acid and its analogues exert anti-inflammatory actions (Kim *et al.*, 1998; Lan *et al.*, 2011). In addition to anti-inflammatory effect, salicylic acid produces an analgesic effect in tail-flick pain models (Dogrul *et al.*, 2007). The main mechanisms of salicylic acid in the production of

anti-inflammation and analgesia are the inhibition of cyclooxygenase system as well as nitric oxide system (Shtivelband *et al.*, 2003; Wang, Brecher, 1999). Moreover, the elevated cytokines such as TNF-α, IL-1, IFN-γ, IL-12, and IL-10 induced by Candida albicans were reduced by salicylic acid (Pereira *et al.*, 2016). Salicylic acid inhibits STAT6 activation or TNF-α-induced NF-kB activation (Katerinaki *et al.*, 2006; Perez-G *et al.*, 2002). However, although the exact site of action of salicylic acid-induced analgesia is not known, Xu *et al.* (2005) have demonstrated that sodium salicylate modulates GABA-induced electrical current in rat dorsal horn neurons.

Based upon those knowledges, an attempt to develop a new analgesic chemical was carried out and we have recently produced a synthetic compound (Lee *et al.*, 2019), which is the hybrid compound (DDIAHB) of epinastine and salicylic acid. Therefore, the present study was designed to examine the possible antinociceptive effects of DDIAHB in various pain models. In addition, we set out to investigate the molecular mechanisms in the production of DDIAHB-induced antinociception. Thus, the effect of DDIAHB on some pain-related signal molecules activated in the spinal cord was examined in the formalin pain model.

MATERIAL AND METHODS

Experimental animals

These experiments were approved by the University of Hallym Animal Care and Use Committee (Registration Number: Hallym 2014-60). All procedures were conducted in accordance with the 'Guide for Care and Use of Laboratory Animals' published by the National Institutes of Health and the ethical guidelines of the International Association for the Study of Pain.

Male ICR mice (MJ Co., Seoul, Korea) weighing 20-25 g were used for all the experiments. Animals were housed 5 per cage in a room maintained at 22 ± 0.5 °C with an alternating 12 h light-dark cycle. Food and water were available *ad libitum*. The animals were allowed to adapt to the laboratory for at least 2 h before testing and were only used once. Experiments were performed during the light phase of the cycle (10:00-17:00).

Synthetic Experiment

All chemical reagents and solvents used in this experiment were obtained from Aldrich, TCI and Alfa aesar, Junsei, Samchun and Burdick & Jackson and were used without purification. All the glassware used in the reaction was dried at 120 °C for more than 12 hours, and most of the reactions were carried out under nitrogen or argon atmosphere.

^{1}H NMR spectrum and ^{13}C NMR spectrum of the compound were analyzed using Varian Gemini 300 (300 MHz). The NMR solvents were CDCl$_3$ and DMSO-d_6 from Cambridge Laboratory. Chemical shift values (δ) are measured from TMS (tetramethylsilane, Me$_4$Si) as internal standard. Glass plates (0.25 mm) preliminarily coated with silica gel 60F$_{254}$ from E. Merck were used as analytical thin layer chromatography (TLC). 70-230 mesh silica gel 60 from E. Merck was used for column chromatography. Mass spectrometry was performed using JEOL's JMS -700.

Synthesis of N-(9,13b-dihydro-1H-dibenzo[c,f] imidazo[1,5-a]azepin-3-yl)-2- hydroxybenzamide (DDIAHB)

DDIAHB was synthesized by the previously reported method as shown in Scheme 1.
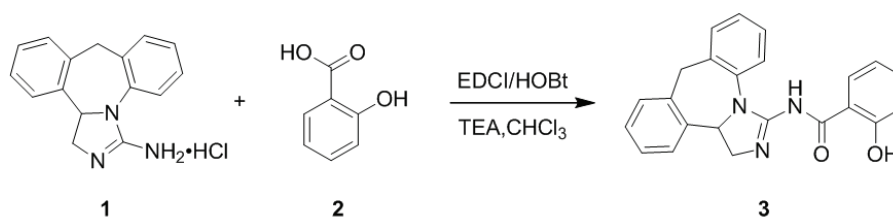
SCHEME 1 - The synthesis of N-(9,13b-dihydro-1H-dibenzo[c,f]imidazo[1,5-a] azepin-3-yl)-2-hydroxybenzamide (DDIAHB). 1. Epinastine (9,13b-dihydro-1H-dibenzo[c,f]imidazo[1,5-a]azepin-3-amine); 2. Salicylic acid; 3. N-(9,13b-dihydro-1H-dibenzo[c,f]imidazo[1,5-a]azepin-3-yl)-2-hydroxybenzamide (DDIAHB).

Intragastric administration

Intragastric administration is typically achieved in conscious mice. Restrain the mice so that its head and body are in a straight, vertical line. Inserted a ball tip needle (18-gauge, 2 inches, Fisher Scientific) into the esophagus and delivering the drug directly into the stomach using KOVAX 1 ml syringe.

Production of streptozotocin-induced diabetic neuropathy model

Diabetic neuropathy animal model was produced using streptozotocin administration. 150 mg/kg (in citrate buffer, pH 4.5) of streptozotocin was intraperitoneal (i.p.) injected once (Sim *et al.,* 2013, Wang *et al.,* 2019). On the 6th day after STZ administration, animals with non-fasting blood glucose concentration above 400 mg/dl were considered to be diabetic and used in the current study. The experiment was performed in 5 weeks after streptozotocin injection.

Production of vincristine-induced chemotherapy-induced peripheral neuropathy model

CIPN animal models were made using vincristine (Linglu *et al*., 2014). Vincristine (0.1 mg/kg) was administered by i.p. once per day for 7 consecutive days. The experiment was performed one day after the last injection with vincristine.

Production of MSU-induced gout pain model

MSU crystals were prepared as described previously (Martinon *et al.,* 2006). One gram of uric acid (Sigma) in 180 ml of 0.01M NaOH was heated to 70°C. NaOH was added as required to maintain the pH between 7.1 and 7.2, and the solution was filtered and incubated at room temperature, with slow and continuous stirring, for 24 h. MSU crystals were kept sterile, washed with ethanol, dried, autoclaved, and resuspended in phosphate-buffered saline (PBS) by sonication. MSU crystals contained <0.005 endotoxin units/ml of endotoxin (Limulus amebocyte lysate endotoxin assay; GenScript). In most experiments (and unless stated otherwise), 0.5 mg of MSU crystals in 10 μl of PBS was injected intraarticularly in one ankle joint, and PBS alone was injected into the contralateral ankle joint. We used Microliter #705 syringes (Hamilton) with 27-gauge needles for all IA injections. Injections were performed with the mice under isoflurane anesthesia, and the quality of IA injection was controlled by assessing the location of MSU crystal deposits histologically on ankle tissue collected 24 h after the injection.

Von-Frey test

Antinociception and Mechanical allodynia were assessed by Von-Frey tests (Bonin, Bories, De Koninck, 2014). For the measurement of the Von-Frey test, mice were individually placed in a clear glass cells with a metal mesh floor allowed to adapt to the testing environment for 30 min, and then Von-Frey filaments (North Coast Medical, Inc., Gilroy, CA, USA) were applied to the plantar surface using an up and down paradigm.

Acetic acid-induced writhing and intraplantar formalin tests

For the writhing test (Koster, Anderson, Beer, 1959), 1% acetic acid was injected by i.p. (10 ml/kg) and then, the animals were immediately placed in an acrylic observation chamber (20 cm high, 20 cm diameter). The number of writhes was counted during 30 min after the injection of acetic acid. A writhe was defined as a contraction of the abdominal muscles accompanied by an extension of the forelimbs and elongation of the body. For the formalin test (Hunskaar, Fasmer, Hole, 1985), 10 μl of 5% formalin was injected subcutaneously under the plantar surface of the left hind paw. Following injection of formalin, the animals were immediately placed in an acrylic observation chamber, and the time spent licking, shaking and biting the injected paw was measured with a stop-watch timer and considered as indication of nociception. The early phase of the nociceptive response normally peaked 0 to 5min, and the last phase 20 to 40 min after formalin injection, representing the direct effect on nociceptors and inflammatory nociceptive responses, respectively (Hunskaar, Hole, 1987). Animals were intragastrically pretreated with DDIAHB (10, 20, 40

or 80 mg/kg) with 30 min prior to performing the acetic acid-induced writhing test or formalin test.

Hot-plate test

Antinociception was determined by the hot-plate paw-licking tests (Eddy, Leimbach, 1953). Mice were individually placed on the 55 ºC hot-plate apparatus (Itic Life Science, Woodland Hills, CA, USA, Model 39 Hot Plate) and then, the reaction time starting from the placement of the mouse on the hotplate to the time of licking the front paw was measured. Basal latency for the hot-plate test was approximately 9 sec.

Protein extraction and western blot

The lumbar section of the spinal cord of mice was dissected. Tissue was washed two times with cold Tris-buffered saline (20mmol/L Trizma base and 137 mmol/L NaCl, pH 7.5). Immediately after washing, tissues were lysed with sodium dodecyl sulfate lysis buffer (62.5 mmol/L Trizma base, 2% w/v sodium dodecyl sulfate, 10% glycerol) containing 0.1mmol/L Na_3VO_4, 3mg/mL aprotinin, and 20 mmol/L NaF. After brief sonication, the concentration of protein was determined with a detergent-compatible protein assay reagent (Bio-Rad Laboratories, Hercules, CA, USA) using bovine serum albumin as the standard. After adding bromophenol blue (0.1% w/v), the proteins were boiled, separated by electrophoresis in 6-10% polyacrylamide gels, and transferred onto a polyvinylidene difluoride membrane (Millipore, Bedford, MA, USA). The membranes were immunoblotted with antibodies iNOS (Abcam, 1:1000), p-STAT3 (Abcam, 1:1000), p-ERK (Cell Signaling Technology, 1:1000), p-P38 (Cell Signaling Technology, 1:1000) and b-actin (Cell Signaling Technology, 1:1000) in a blocking buffer for overnight. Membranes were then washed 4 times with Tris-buffered saline containing 20% Tween-20 (TBST; 10mM Trizma base, pH8.0, 150mM NaCl, and 20% Tween 20) for 20 min and then incubated with the anti-rabbit IgG-horseradish peroxidase conjugate (1:4000) in blocking buffer at room temperature for 1 h. After washing the membranes with TBST for 20 min (4 times), ECL-plus solution (Millipore, Billerica, MA, USA) was added.

The membranes were then exposed to a Luminescent Image Analyzer (LAS-4000, Fuji Film Co., Japan) for the detection of light emission. The specific signals were quantified with the Multi-Gauge Version 3.1 (Fuji Film, Japan) and expressed as the percentage of the control.

Drugs

Salicylic acid, epinastine, monosodium urate, streptozotocin, vincristine were purchased from Sigma Chemical Co. (St. Louis, MO, USA). MSU was dissolved in saline. All drugs were prepared just before use.

Statistical analysis

Statistical analysis was assessed by one-way ANOVA with Bonferroni's post-hoc test using GraphPad Prism Version 8.0.2 for Windows (GraphPad Software, San Diego, CA, USA). p-values less than 0.05 were considered to indicate statistical significance. All values were expressed as the mean ± SEM.

RESULTS

Effect of DDIAHB on pain behavior in writhing, formalin and hot-plate tests.

Intragastric pretreatment with DDIAHB (from 10 to 80 mg/kg) for 30 min attenuated the acetic acid-induced writhing numbers in a dose-dependent manner as shown in Figure 1. In vehicle-treated control group, injection of 5% formalin caused acute, immediate nociceptive formalin responses (i.e., licking/flinching and biting the injected paw) that lasted for 5 min (first phase response) as shown in Figure 2. The second phase nociceptive responses began about 20 min after formalin administration and lasted for about 20 min. In DDIAHB-treated mice (from 10 to 80 mg/kg), the nociceptive behaviors induced by intraplantar injection of formalin were decreased as compared with control group during only second phase (Figure 2). Furthermore, we investigated possible antinociceptive effect of DDIAHB in a thermal pain model such as the hot-plate test. Intragastric administration with DDIAHB (from 10 to

80 mg/kg) increased the latency that the mice lick their paws in a dose-dependent manner as shown in Figure 3.
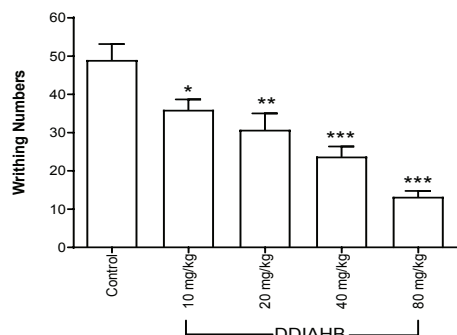
FIGURE 1 - Effect of DDIAHB on the nociceptive response induced by acetic acid. DDIAHB (from 10 to 80 mg/kg) was administered intragastrically and then, 0.25 ml of 1% acetic acid solution was injected intraperitoneally 30 min after DDIAHB treatment. The number of writhing was counted for 30 min following acetic acid injection. The number of animal used for each group was 8-10. Values are mean ± SEM ($^*p < 0.05$; $^{**}p < 0.01$; $^{***}p < 0.001$, compared with control group).
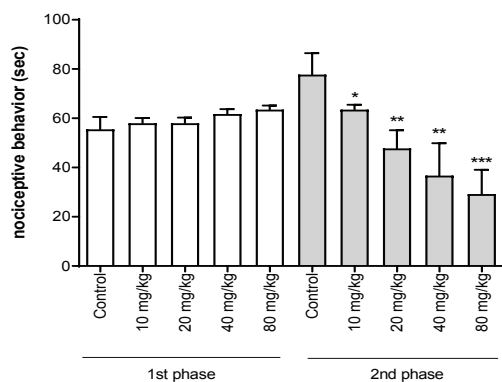
FIGURE 2 - Effect of DDIAHB on the nociceptive response induced by formalin. Mice were administered intragastrically with DDIAHB (from 10 to 80 mg/kg) for 30 min prior to the formalin (5%, 10 µl) injection subcutaneously into the plantar aspect of the left side hindpaw. The cumulative response time of licking, biting and shaking the injected paw was measured during the period of 0-5 min (1st phase) and 20-40 min (2nd phase). The number of animal used for each group was 8-10. Values are mean ± SEM ($^*p < 0.05$; $^{**}p < 0.01$; $^{***}p < 0.001$, compared with control group).
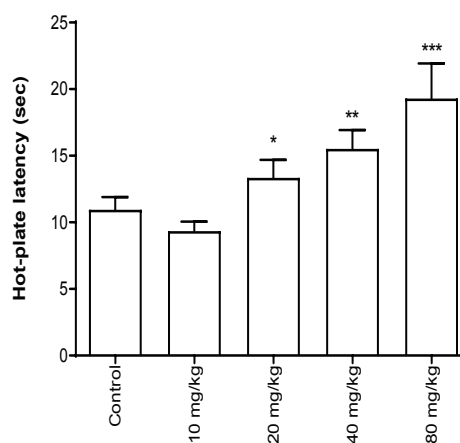
FIGURE 3 - Effect of DDIAHB on the nociceptive response in the hot-plate test. DDIAHB (from 10 to 80 mg/kg) was administered intragastrically and then, after 30 min the mice were put on the surface of hot-plate (55 ºC). The time to licking paws was measured. The number of animal used for each group was 8-10. Values are mean ± SEM ($^*p < 0.05$; $^{**}p < 0.01$; $^{***}p < 0.001$, compared with control group).

Effect of DDIAHB on pain behavior in diabetic neuropathy, chemotherapy-induced peripheral neuropathy, and monosodium urate-induced pain models.

At 5 weeks after the production of streptozotocin-induced diabetic neuropathy model, various doses (from 10 to 80 mg/kg) of DDIAHB was intragastrically administered and the mechanical pain threshold was measured using von-frey filament. As shown in Figure 4, DDIAHB caused reversal of decreased pain threshold in a dose-dependent manner. The antinociceptive effect was manifested up to 3 hrs after DDIAHB administration and the paw withdrawal thresholds were remained higher than that of control level 4 hrs after DDIAHB administration (Figure 4).

As revealed in Figure 5, repeated i.p. administrations with vincristine caused reduction of threshold of mechanical stimulation as manifested by Von-frey filament test. The intragastric treatment with DDIAHB (from 10 to 80 mg/kg) dose-dependently produced antinociceptive effect in the mechanical stimulation as manifested by Von-frey test. The antinociceptive effect was manifested up to 3 hrs after DDIAHB administration

and returned to the control level 4 hrs after DDIAHB administration (Figure 5).

Monosodium urate-induced pain model was produced by injecting monosodium urate into the ankle of the mice. At 24 hrs after monosodium urate injection, various doses (from 10 to 80 mg/kg) of DDIAHB was intragastrically administered and the mechanical pain threshold was measured using von-frey filament. As shown in Figure 6, DDIAHB caused reversal of decreased pain threshold in a dose-dependent manner after 2 hr of treatment. However, only the highest dose (80 mg/kg) of DDIAHB produced an antinociceptive effect either after 1 or 3 hr.
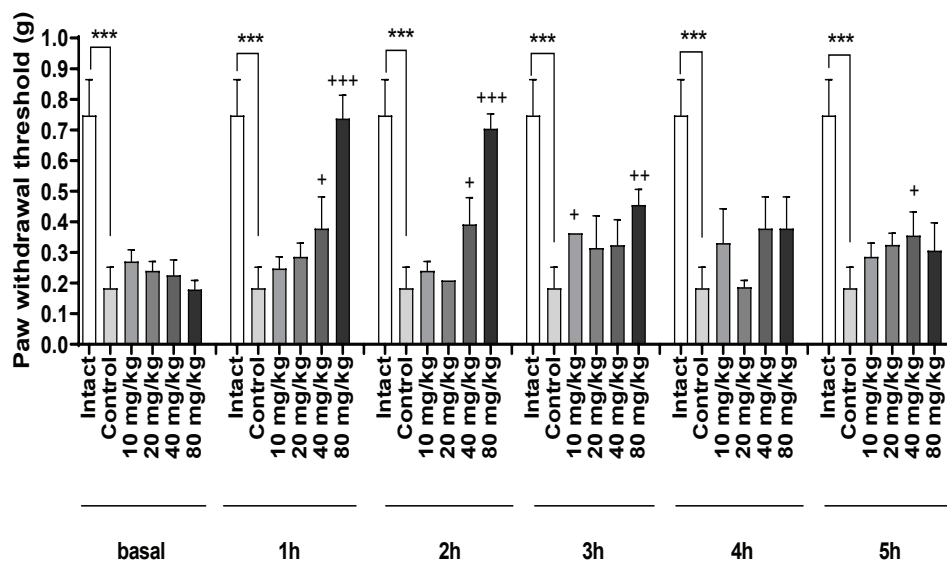
FIGURE 4 - Antinociceptive effect of DDIAHB in diabetic neuropathy model. To produce diabetic neuropathy animal model, streptozotocin (150 mg/kg) was administered i.p. once. The experiment was performed in 5 weeks after streptozotocin injection. The number of animal used for each group was 8-10. Values are mean $\pm$ SEM. (***$p < 0.001$, compared with intact group; $^{+}p < 0.05$, $^{++}p < 0.01$, $^{+++}p < 0.001$, compared with control group).
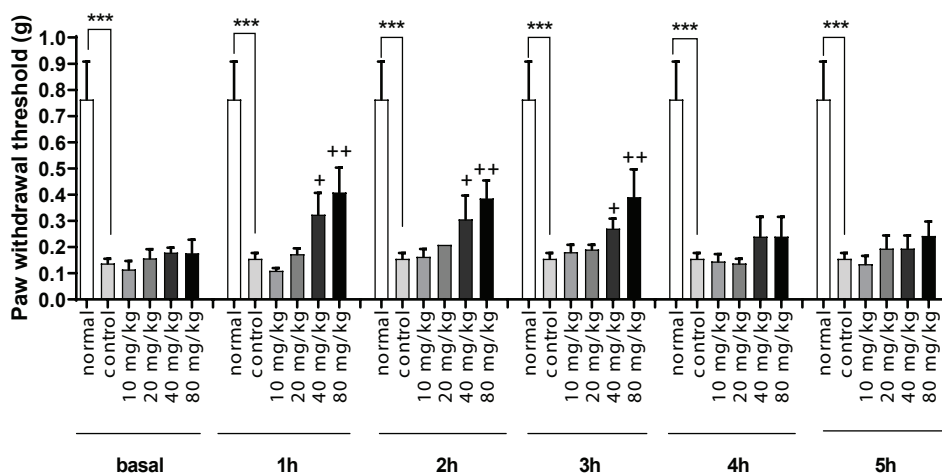
FIGURE 5 - Antinociceptive effect of DDIAHB in chemotherapy-induced peripheral neuropathy model. To produce chemotherapy-induced peripheral neuropathy animal model, 0.1 mg/kg of vincristine was administered i.p. once per day for 7 consecutive days. The experiment was performed one day after the last injection with vincristine. The number of animal used for each group was 8-10. Values are mean $\pm$ SEM (***$p < 0.001$, compared with intact group; $^{+}p < 0.05$, $^{++}p < 0.01$, compared with control group).
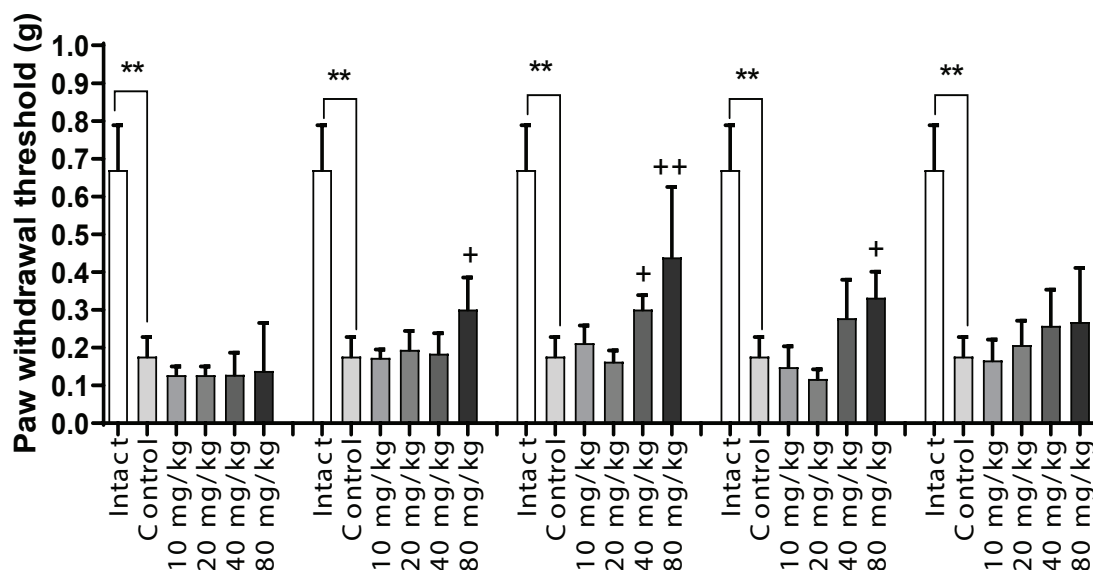
FIGURE 6 - Antinociceptive effect of DDIAHB in monosodium urate-induced pain model. 0.5 mg of MSU crystals in 10 µl of PBS was injected intraarticularly in one ankle joint, and PBS alone was injected into the contralateral ankle joint under isoflurane anesthesia. The experiment was performed at 24 hr after the MSU injection. The number of animal used for each group was 8-10. Values are mean ± SEM ($^{**}p < 0.01$, compared with intact group; $^{+}p < 0.05$, $^{++}p < 0.01$, compared with control group).

Changes of phosphorylated iNOS, STAT3, ERK, and P38 proteins in the spinal cord by DDIAHB in the formalin test.

To examine whether iNOS, p-STAT3, p-ERK, and p-P38 protein were changed in the spinal cord after formalin injection is occur, the proteins were extracted from dissected lumbar spinal cord at 30 min after formalin injection. As shown in Figure 7 and 8, formalin injection caused up-regulations of iNOS, p-STAT3, p-ERK, and p-P38 expression in the spinal cord. In addition, intragastric administration with DDIAHB (80 mg/kg) attenuated formalin-induced iNOS, p-STAT3, p-ERK, and p-P38 levels (Figures 7 and 8).

A

A

B

B
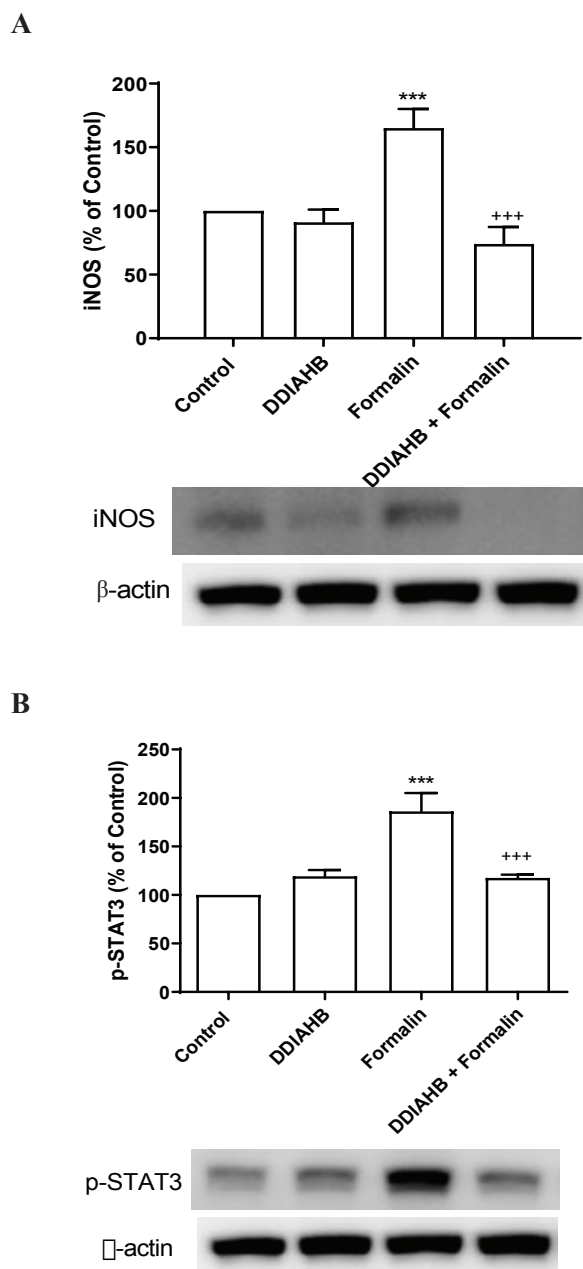
FIGURE 7 - Changes of iNOS and phosphorylated STAT3 proteins in the spinal cord by DDIAHB in the formalin test. To examine if a change in iNOS and p-STAT3 expression in the spinal cord after formalin injection, the proteins were extracted from dissected lumbar spinal cord 30 min after formalin injection for Western blot analysis. The number of animals in each group is 6. β-Actin (1:1000 dilution) was used as an internal loading control. Signals were quantified with the use of laser scanning densitometry and expressed as a percentage of the control. Values are mean ± SEM (***$p < 0.001$, compared to control group; +++$p < 0.001$, compared to formalin-treated group).
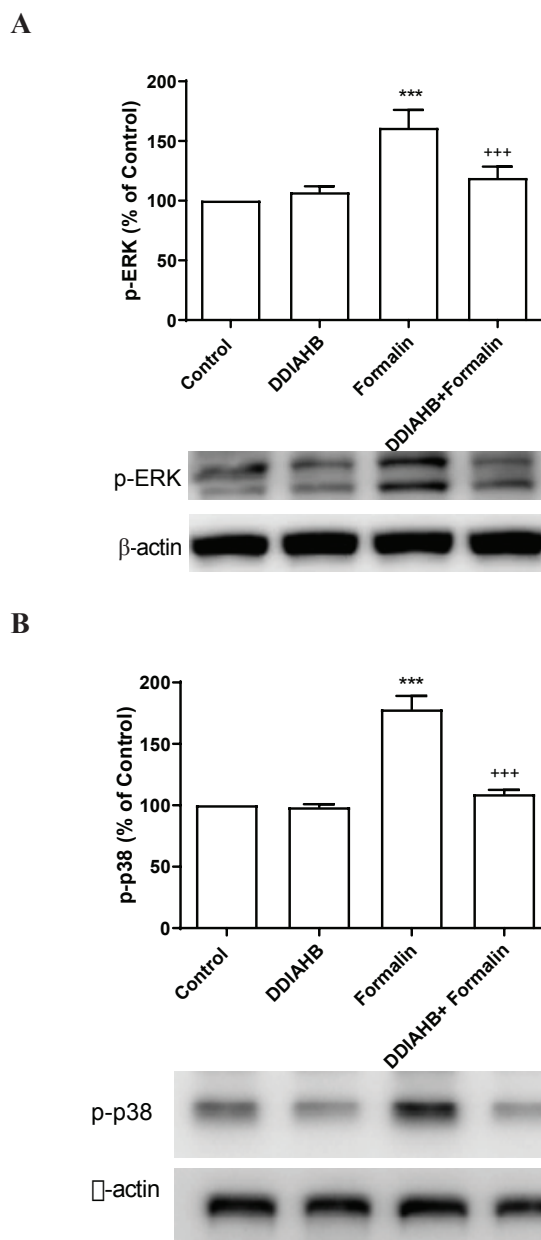
FIGURE 8 - Changes of phosphorylated ERK and P38 proteins in the spinal cord by DDIAHB in the formalin test. To examine if a change in p-ERK and p-P38 expression in the spinal cord after formalin injection, the proteins were extracted from dissected lumbar spinal cord 30 min after formalin injection for Western blot analysis. The number of animals in each group is 6. β-Actin (1:1000 dilution) was used as an internal loading control. Signals were quantified with the use of laser scanning densitometry and expressed as a percentage of the control. Values are mean ± SEM (***$p < 0.001$, compared to control group; +++$p < 0.001$, compared to formalin-treated group).

DISCUSSION

We observed in the present study that DDIAHB exerts antinociceptive effect in various pain models. Intragastric administration with DDIAHB was effective in reducing the writhing number in the writhing pain test, indicating that DDIAHB appears to be effective in chemically-induced abdominal pain. In addition, DDIAHB reduced the pain behavior observed during the 2nd phase in the formalin test, indicating that DDIAHB is also effective in relieving the inflammation-induced pain behavior induced by formalin injection into the plantar of the hind-paw of mice. Furthermore, we further tried to characterize of DDIAHB-induced antinociceptive effect in thermally-stimulated pain model. We found that DDIAHB was also effective to increase the latency that mice lick their paws as manifested in the hot-plate test, suggesting that DDIAHB reduces thermally-oriented nociception.

The pain behavior observed during the first phase is mostly due to the direct stimulation of nociceptors, whereas the pain behaviors observed during the second phase involves both inflammatory mechanisms and central sensitization within the dorsal horn, suggesting that pain behaviors observed during the first and second phases are differentially regulated (Shibata *et al.,* 1989; Tjølsen A *et al.,* 1992). Our results indicate that DDIAHB is mostly effective in relieving the inflammation-induced pain behavior induced by intraplantar injection formalin.

Previously, we examined the in vitro anti-inflammatory effect of epinastine-NSAIDs hybrid drugs (Lee *et al.,* 2019; Woo *et al.,* 2020), DDIAHB displayed a better potency compared to other hybrid compounds in the inhibitory effect against NO production. Moreover, in our previous study, aspirin at doses of 100mg/kg or acetaminophen at doses of 200 mg/kg significantly attenuated pain behavior induced by formalin in the second phase (Kwon *et al.,* 2005). Especially, in the present study, DDIAHB reduces antinociception in formalin-induced inflammatory models only at a very low dose of 10 mg/kg. Based on these results, DDIAHB may be applied as an effective antinociceptive candidate.

To examine if DDIAHB is also effective in modulating mechanically-induced pain, we have produced diabetic neuropathy, chemically-induced peripheral neuropathy, and monosodium urate-induced pain models. Five weeks after the production of streptozotocin-induced diabetic neuropathy model, we examined the possible antinociceptive effect of DDIAHB and found that DDIAHB was effective in relieving diabetic-induced neuropathy. We also produced chemically-induced peripheral neuropathy models by repeated injection of vincristine, one of anticancer drugs. We found that intragastric administration with DDIAHB caused the reversal of decreased pain threshold in vincristine-induced peripheral neuropathy, suggesting that DDIAHB is also effective in relieving chemically-induced peripheral neuropathy. Several previous studies have demonstrated that MSU is used as gout pain model (Dalbeth, Haskard, 2005; Geronikolou, 2014). In the present study, we confirmed that MSU treatment caused a reduction of mechanical pain threshold as measured by Von-Frey stimulation of plantar of the mouse. DDIAHB caused the reversal of decreased threshold of MSU-induced pain. Our results further demonstrate that DDIAHB is also effective in relieving the mechanically-induced pain behavior, suggesting that DDIAHB may be a good candidate for relieving gout-induced pain.

Numerous studies have previously demonstrated that iNOS, STAT3, CREB, ERK and P38 proteins are closely associated with pain transmission (Jin *et al*., 2003; Lee *et al*., 2012; Nemoto *et al*., 2015; Wang *et al*., 2018; Wang, Li, Guo, 2016). For example, iNOS, p-STAT3, p-ERK, and p-P38 expressions in the spinal cord or dorsal root ganglia are up-regulated in various types of pain models (Cao *et al*., 2005; Crown *et al*., 2008; Descalzi *et al*., 2012). The up-regulations of iNOS, p-STAT3, p-ERK and p-P38 expressions in formalin-induced pain model were observed in the present study. Furthermore, we found in the present study that intragastric pretreatment with DDIAHB almost abolished the spinal iNOS, p-STAT3, p-ERK, and p-P38 expressions induced by formalin injection, suggesting that the reduction of nociception by DDIAHB treatment in formalin pain model appears to be mediated, at least, by the reductions of iNOS, p-STAT3, p-ERK, and p-P38 levels in the spinal cord. However, the direct effect on enzyme activity of iNOS, and enzyme activities for phosphorylating STAT3, ERK, and P38 proteins should be carried out in the future.

CONFLICT OF INTEREST

The authors declare that they have no conflict of interest.

ACKNOWLEDGEMENTS

REFERENCES

Adamus W, Oldigs-Kerber J, Lohmann H. Pharmacodynamics of the new H1-antagonist 3-amino-9, 13b-dihydro-1H-dibenz [c, f] imidazo [1, 5-a] azepine hydrochloride in volunteers. Arzneimittelforschung. 1987;37(5):569-572.

Bonin RP, Bories C, De Koninck Y. A simplified up-down method (SUDO) for measuring mechanical nociception in rodents using von Frey filaments. Mol Pain. 2014;10(1):26.

Cao JL, Ding HL, He JH, Zhang LC, Duan SM, Zeng YM. The spinal nitric oxide involved in the inhibitory effect of midazolam on morphine-induced analgesia tolerance. Pharmacol Biochem Behav. 2005;80(3):493-503.

Crown ED, Gwak YS, Ye Z, Johnson KM, Hulsebosch CE. Activation of p38 MAP kinase is involved in central neuropathic pain following spinal cord injury. Exp Neurol. 2008;213(2):257-67.

Dalbeth N, Haskard D. Mechanisms of inflammation in gout. Rheumatology (Oxford). 2005;44(9):1090-1096.

Descalzi G, Fukushima H, Suzuki A, Kida S, Zhuo M. Genetic enhancement of neuropathic and inflammatory pain by forebrain upregulation of CREB-mediated transcription. Mol Pain. 2012;8:90.

Dogrul A, Gülmez SE, Deveci MS, Gul H, Ossipov MH, Porreca F, et al. The local antinociceptive actions of nonsteroidal antiinflammatory drugs in the mouse radiant heat tail-flick test. Anesth Analg. 2007;104(4):927-935.

Eddy NB, Leimbach D. Synthetic analgesics. II. Dithienylbutenyl-and dithienylbutylamines. J Pharmacol Exp Ther. 1953;107(3):385-393.

Geronikolou SA. Treatment of gout in a recently published 9th century manuscript of Rhazes. Vesalius. 2014;20(2):95-98.

Hung AL, Lim M, Doshi TL. Targeting cytokines for treatment of neuropathic pain. Scand J Pain. 2017;17:287-293.

Hunskaar S, Fasmer OB, Hole K. Formalin test in mice, a useful technique for evaluating mild analgesics. J Neurosci Methods. 1985;14(1):69-76.

Hunskaar S, Hole K. The formalin test in mice: dissociation between inflammatory and non-inflammatory pain. Pain. 1987;30(1):103-114.

Jin SX, Zhuang ZY, Woolf CJ, Ji RR. p38 mitogen-activated protein kinase is activated after a spinal nerve ligation in spinal cord microglia and dorsal root ganglion neurons and contributes to the generation of neuropathic pain. J Neurosci. 2003;23(10):4017-22.

Kanai K-i, Asano K, Watanabe S, Kyo Y, Suzaki H. Epinastine hydrochloride antagonism against interleukin-4-mediated T cell cytokine imbalance in vitro. Int Arch Allergy Immunol. 2006;140(1):43-52.

Katerinaki E, Haycock JW, Lalla R, Carlson KE, Yang Y, Hill RP, et al. Sodium salicylate inhibits TNF-α-induced NF-κB activation, cell migration, invasion and ICAM-1 expression in human melanoma cells. Melanoma Res. 2006;16(1):11-22.

Khan J, Hassun H, Zusman T, Korczeniewska O, Eliav E. Interleukin-8 levels in rat models of nerve damage and neuropathic pain. Neurosci Lett. 2017;657:106-112.

Kim HM, Lee EH, Shin TK, Chung CK, An N. Inhibition of the induction of the inducible nitric oxide synthase in murine brain microglial cells by sodium salicylate. Immunology. 1998;95(3):389.

Kohyama T, Takizawa H, Akiyama N, Sato M, Kawasaki S, Ito K. A novel antiallergic drug epinastine inhibits IL-8 release from human eosinophils. Biochem Biophys Res Commun. 1997;230(1):125-128.

Koster R, Anderson M, Beer EJ. Acetic acid for analgesic screening. Fed proc. 1959;18:412.

Kwon MS, Shim EJ, Seo YJ, Choi SS, Lee JY, Lee HK, et al. Effect of aspirin and acetaminophen on proinflammatory cytokine-induced pain behavior in mice. Pharmacol. 2005;74(3):152-156.

Lan X, Liu R, Sun L, Zhang T, Du G. Methyl salicylate 2-O-β-D-lactoside, a novel salicylic acid analogue, acts as an anti-inflammatory agent on microglia and astrocytes. J Neuroinflammation. 2011;8(1):98.

Lanier BQ, Finegold I, D'Arienzo P, Granet D, Epstein AB, Ledgerwood GL. Clinical efficacy of olopatadine vs epinastine ophthalmic solution in the conjunctival allergen challenge model. Curr Med Res Opin. 2004;20(8):1227-1233.

Lee JM, Damodar K, Lee Y, Lee J, Jeon SH, Lee JT. Synthesis and Biological Assay of Hybrids Between Epinastine and Salicylic Acid as Promising Nitric Oxide Production Inhibitors. Bull Korean Chem Soc. 2019;40:735-740.

Lee MJ, Jang M, Jung HS, Kim SH, Cho IH. Ethyl pyruvate attenuates formalin-induced inflammatory nociception by inhibiting neuronal ERK phosphorylation. Mol Pain. 2012;8:40.

Linglu D, Yuxiang L, Yaqiong X, Ru Z, Lin M, Shaoju J, et al. Antinociceptive effect of matrine on vincristine-induced neuropathic pain model in mice. Neurol Sci. 2014;35(6):815-821.

Mah FS, Rosenwasser LJ, Townsend WD, Greiner JV, Bensch G. Efficacy and comfort of olopatadine 0.2% versus epinastine 0.05% ophthalmic solution for treating itching and redness induced by conjunctival allergen challenge. Curr Med Res Opin. 2007;23(6):1445-1452.

Martinon F, Pétrilli V, Mayor A, Tardivel A, Tschopp J. Gout-associated uric acid crystals activate the NALP3 inflammasome. Nature. 2006;440(7081):237.

Mizuguchi H, Hatano M, Matsushita C, Umehara H, Kuroda W, Kitamura Y et al. Repeated pre-treatment with antihistamines suppresses transcriptional up-regulations of histamine H-1 receptor and interleukin-4 genes in toluene-2, 4-diisocyanate-sensitized rats. J Pharmacol Sci. 2009;109(2):324-324.

Mollanazar NK, Smith PK, Yosipovitch G. Mediators of chronic pruritus in atopic dermatitis: getting the itch out? Clin Rev Allergy Immunol. 2016;51(3):263-292.

Nemoto W, Ogata Y, Nakagawasai O, Yaoita F, Tanado T, Tan-No K. The intrathecal administration of losartan, an AT1 receptor antagonist, produces an antinociceptive effect through the inhibiton of p38 MAPK phosphorylation in the mouse formalin test. Neurosci Lett. 2015;585:17-22.

Otsuka A, Honda T, Doi H, Miyachi Y, Kabashima K. An H1-histamine receptor antagonist decreases serum interleukin-31 levels in patients with atopic dermatitis. Br J Dermatol. 2011;164(2):455-456.

Otsuka A, Tanioka M, Nakagawa Y, Honda T, Ikoma A, Miyachi Y, et al. Effects of cyclosporine on pruritus and serum IL-31 levels in patients with atopic dermatitis. Eur J Dermatol. 2011;21(5):816-817.

Pereira PAT, Bini D, Bovo F, Faccioli LH, Monteiro MC. Neutrophils influx and proinflammatory cytokines inhibition by sodium salicylate, unlike aspirin, in Candida albicans-induced peritonitis model. Folia Microbiol (Praha). 2016;61(4):337-346.

Perez-G M, Melo M, Keegan AD, Zamorano J. Aspirin and salicylates inhibit the IL-4-and IL-13-induced activation of STAT6. J Immunol. 2002;168(3):1428-1434.

Shibata M, Ohkubo T, Takahashi H, Inoki R. Modified formalin test: characteristic biphasic pain response. Pain. 1989;38(3):347-352.

Shtivelband M, Juneja H, Lee S, Wu K. Aspirin and salicylate inhibit colon cancer medium-and VEGF-induced endothelial tube formation: correlation with suppression of cyclooxygenase-2 expression. J Thromb Haemost. 2003;1(10):2225-2233.

Sim YB, Park SH, Kang YJ, Kin SS, Kim CH, Kim SJ et al. Repaglinide, but not nateglinide administered supraspinally and spinally exerts an anti-diabetic action in d-glucose fed and streptozotocin-treated mouse models. Korean J Physiol Pharmacol. 2013;17(6):493–497.

Tjølsen A, Berge O-G, Hunskaar S, Rosland JH, Hole K. The formalin test: an evaluation of the method. Pain. 1992;51(1): 5-17.

Wang B, Liu S, Fan B, Xu X, Chen Y, Lu R et al. PKM2 is involved in neuropathic pain by regulating ERK and STAT3 activation in rat spinal cord. J Headache Pain. 2018;19(1):7.

Wang K, Song F, Wang H, Wang JH, Sun Y. Quetiapine Attenuates the Neuroinflammation and Executive Function Deficit in Streptozotocin-Induced Diabetic Mice. Mediators Inflamm. 2019;2019:1236082.

Wang S, Li A, Guo S. Ligustrazine attenuates neuropathic pain by inhibition of JAK/STAT3 pathway in a rat model of chronic constriction injury. Pharmazie. 2016;71(7):408-412.

Wang Z, Brecher P. Salicylate inhibition of extracellular signal-regulated kinases and inducible nitric oxide synthase. Hypertension. 1999;34(6):1259-1264.

Woo HR, Damodar K, Lee Y, Lim SS, Jeon S H, Lee JT. Discovery of epinastine-NSAID hybrids as potential anti-inflammatory agents: Synthesis and in vitro nitric oxide production inhibitory activity study. J Korean Chem Society, 2020;64(2):79-83.

Xu H, Gong N, Chen L, Xu TL. Sodium salicylate reduces gamma aminobutyric acid-induced current in rat spinal dorsal horn neurons. Neuroreport. 2005;16(8):813-816.